Available online at www.sciencedirect.com
SCIENCE DIRECT®
Journal of Membrane Science 228 (2004) 5–16
journal of MEMBRANE SCIENCE
www.elsevier.com/locate/memsci

Experimental study of desalination using direct contact membrane distillation: a new approach to flux enhancement

Tzahi Y. Cath, V. Dean Adams, Amy E. Childress*

Department of Civil Engineering, University of Nevada, Reno, NV 89557, USA

Received 7 April 2003; received in revised form 7 August 2003; accepted 4 September 2003

Abstract

New membrane distillation configurations and a new membrane module were investigated to improve water desalination. The performances of three hydrophobic microporous membranes were evaluated under vacuum enhanced direct contact membrane distillation (DCMD) with a turbulent flow regime and with a feed water temperature of only 40 °C. The new configurations provide reduced temperature polarization effects due to better mixing and increased mass transport of water due to higher permeability through the membrane and due to a total pressure gradient across the membrane. Comparison with previously reported results in the literature reveals that mass transport of water vapors is substantially improved with the new approach. The performance of the new configuration was investigated with both NaCl and synthetic sea salt feed solutions. Salt rejection was greater than 99.9% in almost all cases. Salt concentrations in the feed stream had only a minor effect on water flux. The economic aspects of the enhanced DCMD process are briefly discussed and comparisons are made with the reverse osmosis (RO) process for desalination.

Keywords: Membrane distillation; Direct contact membrane distillation; Temperature polarization; Desalination; Low temperature evaporation

1. Introduction

Membrane distillation (MD) is a membrane process that has long been investigated in small scale laboratory studies and has the potential to become a viable tool for water desalination [1–10]. MD is a separation process that combines simultaneous mass and heat transfer through a hydrophobic microporous membrane. Mass transfer in this process is carried out by evaporation of a volatile solute or a volatile solvent (water), when the solute is non-volatile. The driving force for mass transfer in the process is vapor pressure difference across the membrane. Direct contact membrane distillation (DCMD) is one of four basic configurations of MD. In this configuration a feed solution at elevated temperature is in contact with one side of the membrane and colder water is in direct contact with the opposite side of the membrane (Fig. 1); it is mainly the temperature difference between the liquids, and to some extent their solute concentration, that induces the vapor pressure gradient for mass transfer. Mass transfer in DCMD is a three-step process involving: (1) diffusive transport from the feed stream to the membrane interface, (2) combined diffusive and convective transport of the vapors through the membrane pores, and (3) condensation of the vapors on the membrane interface on the product side of the membrane.

1.1. Energetic inefficiencies in MD

There are three major energetic inefficiencies in MD [11]. The first is the temperature polarization across the membrane [12–15], the second is the resistance to vapor flow through the membrane due to the presence of trapped air in the pores [16–18], and the third is a conductive heat loss through the membrane [19–22]. The majority of previous investigations focused on the effects of either temperature polarization or resistance to vapor flow in the pores on the performance of MD. In the current study, both of these inefficiencies are confronted simultaneously in one system, and in doing so, the mass transfer of water vapors through the membrane is enhanced.

1.1.1. Temperature polarization effects

Heat in MD is transported across the system through two major routes [8]. Transport of the latent heat of evaporation

* Corresponding author. Tel.: +1-775-784-6942; fax: +1-775-784-1390.
E-mail address: amyec@unr.edu (A.E. Childress).

0376-7388/$ – see front matter © 2003 Elsevier B.V. All rights reserved.
doi:10.1016/j.memsci.2003.09.006

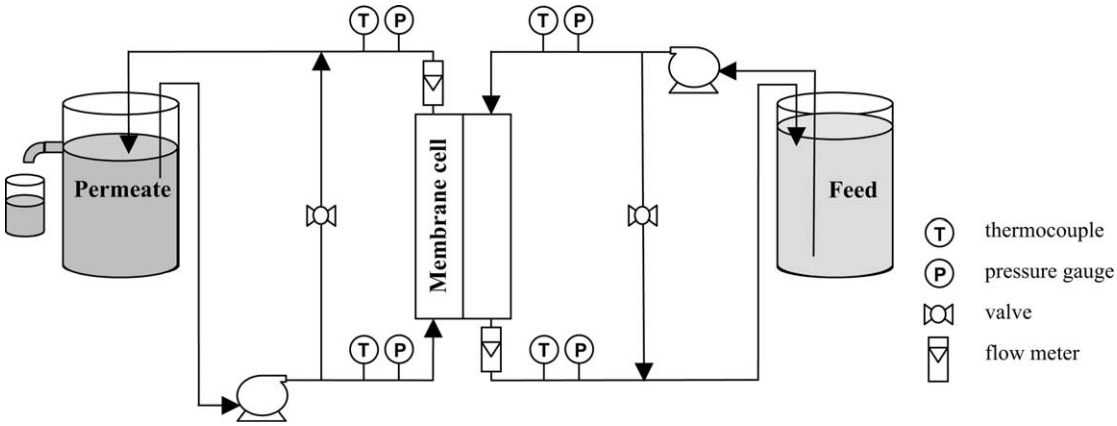

Fig. 1. Common DCMD apparatus.

jointly with the vapors across the membrane is one form of heat transfer that cannot be eliminated since it directly serves the purpose of the process—evaporation. On the contrary, conductive heat transport across the thin membrane and through the boundaries of the system is a source of inefficiency because this heat is no longer available for use in evaporation. Use of heat exchangers to recover the lost heat at small temperature differences is expensive and might be prohibitive for commercial development of the process.

Both paths of heat transfer are the source of thermal boundary layers developed on the faces of the membrane. Heat transfer across the thermal boundary layer frequently limits the mass transfer in MD [23]—further reducing the supply of heat for evaporation to the feed–membrane interface. The ratio of useful energy for mass transfer of vapors to the total energy invested in the process is the temperature polarization coefficient (TPC) which is commonly defined as [12]:

$$\mathrm{TPC} = \frac{T_{\mathrm{mf}} - T_{\mathrm{mp}}}{T_{\mathrm{f}} - T_{\mathrm{p}}} \quad (1)$$

where T_{mf} is the interfacial feed temperature, T_{mp} the interfacial permeate temperature, T_{f} the bulk feed temperature, and T_{p} is the bulk permeate temperature. A schematic drawing of temperature polarization in MD is shown in Fig. 2. Given that the evaporation and condensation rates depend on the interfacial temperatures (not the bulk temperatures) and because the vapor pressure driving force is primarily a function of temperature, it is desired that the difference between T_{mf} and T_{mp} be as high as possible. In other words, the TPC should be as close to unity as possible. However, most often the TPC is lower than unity and varies between 0.2 and 0.9 [24], depending on the membrane module configuration.

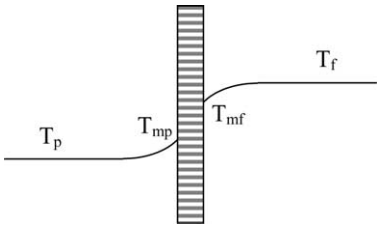

Fig. 2. Temperature polarization in MD.

The TPC can be increased by improving membrane module design and/or operation parameters. For example, by working at a turbulent flow regime on both the feed and permeate sides, the thermal boundary layers can be reduced, thereby increasing T_{mf} and decreasing T_{mp}. Better mixing can be achieved either by increasing flow rates [25,26] or by using mesh spacers in the channels to induce turbulent flow [27]. Most studies show positive dependence of flux on feed flow rate, yet, Lawson and Lloyd [25,26] were pioneers in showing the extent to which mixing of the streams affects the flux in MD. In their DCMD module, the feed and permeate streams were flowing at high speed in narrow rectangular channels. The module was operated at very high Reynolds Numbers (up to 25,000), and produced exceptionally high fluxes. The only drawback of the system was that the adverse effects of partial air pressure in the pores on mass transfer and conductive heat loss in the system were not considered. Martinez-Diez and Vazquez-Gonzalez [27] investigated the effect of turbulence-enhancing spacers in the flow channels of a DCMD system. Though the Reynolds numbers could not be defined for the flow in the channels, it was qualitatively shown that higher fluxes could be achieved with enhanced mixing. However, it is important to note that while mixing devices (e.g., spacers) efficiently promote heat transfer to the membrane surface, they increase the pressure drop in the channel, cause additional heat transfer resistance in the liquid [7], and possibly reduce the surface area available for evaporation.

1.1.2. Resistance to mass transfer through the membrane in MD

Vapors transported through pores in DCMD are subject to molecular resistance by the air trapped in the pores as well as to resistance imposed by the physical structure of the pore [11]. Several approaches to overcome these resistances were studied in the last two decades. In the early 1980s, Schneider and van Gassel [28] introduced the idea

of degasification of the working fluids in DCMD systems to reduce the partial pressure of air in the membrane pores. It was demonstrated that by operating the permeate stream under vacuum, flux could be more than doubled. However, due to other operating conditions and mainly due to the specific tubular membranes used in their study, fluxes were relatively low (below 5 l/(m^2 h) for feed and permeate temperatures of 40 and 20 °C, respectively). Although this study suggested a very simple method to operate DCMD in an efficient way, Schneider's approach was not further developed.

In another approach, which was intensively investigated in the early 1990s by Schofield et al. [16,17], both sides of the system (both the feed and permeate streams) were placed under vacuum to control the partial pressure of air in the pores. Using a flat sheet membrane, it was demonstrated that flux increased with increasing deaeration. However, the permeate liquid in the membrane cell was almost stagnant and resulted in a low TPC in the system, thereby overshadowing the increase in flux due to pressure reduction. Furthermore, it was concluded that module design is very important in improving the performance of DCMD.

Membrane properties such as porosity, pore size, tortuosity, and membrane thickness play a significant role in dictating the resistance to mass transfer through microporous membranes in MD [18,29,30]. Furthermore, studies [31–34] have shown that the relationships between the membrane properties (not only the properties by themselves) as well as membrane conditions (e.g., compaction, wetting, etc.) are important for efficient operation. Therefore, selection of an appropriate membrane that poses the least resistance to mass transfer is crucial.

1.1.3. Conductive heat loss through the membrane

Conductive heat loss through the membrane can rarely be controlled because of the trade off between a thick membrane for better heat insulation and a thin membrane for reduced mass flow resistance in the membrane [24]. Increasing the porosity of the membrane is a possible solution since the air in the pores has better insulation properties than the polymeric material of the membrane and since increased porosity also increases the available surface area for evaporation. However, microporous membranes with porosities of 80% and higher already exist [24] and further improvement may only be achieved when nanotube technology matures [35]. Alternative materials for membranes are also not expected to improve the process because the requirement for hydrophobicity is strict and most hydrophobic polymers have relatively similar heat conductivities [36,37].

1.2. Additional design considerations for MD modules

Two additional interrelated design aspects need to be carefully considered for MD modules—the pressure drop along the module and the liquid entry pressure of water (LEPW). Pressure drop is a natural phenomenon that happens when fluids are flowing in channels and is due to a resistance to flow imposed by the walls and the fluid itself [38]. In order to maintain a flow in a channel, a minimum pressure (that might be significant and detrimental in MD) must be maintained at the entrance to the flow channel. The pressure drop (ΔP) along a channel of length L is expressed as:

$$\Delta P = f\frac{L}{d}\rho\frac{u^2}{2} \tag{2}$$

where f is the friction factor, d the hydraulic diameter of the flow channel, ρ the fluid density, and u is the fluid velocity [38].

While Reynolds number, a measure of mixing intensity, is a linear function of velocity, pressure drop is a function of the second power of velocity (Eq. (2)), and therefore, an optimization process must be carried out in designing the dimensions and hydraulics of the membrane cell. In the current investigation, a spreadsheet was developed to assist in determining the membrane cell configuration that will maximize mixing and membrane surface area but will ensure low pressure and pressure drop in the flow channel. The program was constrained by restrictions on channel width, auxiliary equipment capacity, and maximum allowable pressure in the system. During the design stage it became apparent that the level of mixing is limited by the strong relationship between flow velocity and pressure and that flow velocity cannot be indefinitely increased in MD applications without compromising on surface area or area-to-volume ratio.

LEPW is the minimum pressure at which water will overcome the hydrophobic forces of the membrane and will penetrate the pores. LEPW is a function of the properties of the membrane, the liquid, and the reaction between them, as given by the Laplace (Cantor) equation [23]:

$$P_{\text{liquid}} - P_{\text{vapor}} = \Delta P_{\text{interface}} = \frac{-2B\gamma_{\text{L}}\cos\theta}{r_{\max}} < \text{LEPW} \tag{3}$$

where B is a geometric factor determined by pore structure, γ_{L} the liquid surface tension, $r_{\max}$ the largest pore size, and θ is the liquid–solid contact angle. Garcia-Payo et al. [34] have demonstrated that for membranes with pore sizes of approximately 0.2 μm, the LEPW would be 200–400 kPa, while for membranes with pore sizes of 0.45 μm the LEPW might be as low as 100 kPa. In operating MD at high Reynolds numbers, pressures can easily exceed the LEPW and result in penetration of water into the pores and termination of the evaporation process. In the current study, design of the membrane module took into account both maximization of mixing and minimization of pressure in the system to prevent flooding of the pores and to achieve better performance of DCMD for desalination.

1.3. Objectives

The main objective of this study was to evaluate the synergetic effects of operating DCMD under the combined conditions of high flow rates for improving heat transfer and low pressure in the pores for reducing membrane resistance

to mass transfer. The effects of membrane properties, pressures, flow rates, and feed salinity on the performance of the process were investigated. The aim was to maximize water flux and salt rejection while utilizing a low temperature feed stream—similar to one that can easily be obtained from waste heat sources. To do this, a new membrane cell was designed and four membranes were tested. The new cell was tested in three configurations. The first was a traditional configuration in which the streams were pumped *into* the membrane cell countercurrently. The purpose of this test was to acquire baseline data on the performance of the newly designed membrane cell—performance that was later compared with the new configurations as well as with earlier investigations of DCMD. The second was a new configuration (DCMD/vacuum) in which the permeate stream is pumped *out* of the membrane cell so that vacuum was induced on the permeate side. This configuration was used to determine to what extent the performance could be improved by simultaneous reductions in energetic inefficiencies. The third configuration tested was a configuration in which both the feed and permeate streams were pumped out of the membrane cell—inducing vacuum on both sides of the membrane (DCMD/vacuum–vacuum). The main objective in testing this configuration was to separate the effect of mass transport due to the total pressure gradient across the membrane and the effect of reduced resistance to mass transport in the pores due to the partial elimination of the air film in the pores. It was also used to compare the performance of this configuration with early studies that investigated vacuum in the membrane pores.

2. Material and methods

2.1. Microporous membranes

Four hydrophobic, microporous membranes were acquired from Osmonics Corp. (Minnetonka, MN) for this investigation. Three of the membranes are composite membranes having a thin polytetrafluoroethylene (PTFE) active layer and a polypropylene (PP) support sublayer. The other membrane is a symmetric, isotropic membrane made from pure PP. The pore size, porosity, and thickness of each of the membranes used in this study are given in Table 1.

2.2. DCMD test unit

The performance of the DCMD processes under various solution chemistries and operating conditions was evaluated using a closed-loop bench-scale membrane test unit. The traditional configuration of the DCMD apparatus is shown in Fig. 1. New configurations were created and tested by altering the positions of the pumps, membrane cell, and valves to allow the streams on one or both sides of the membrane to flow under negative pressure (vacuum). Fig. 3 illustrates the new configurations tested in this investigation (b and c) alongside the traditional DCMD configuration (a).

A new membrane cell was designed to hold a flat-sheet membrane under moderate pressure gradients without a physical support. As indicated earlier, design considerations included maximization of mixing and minimization of pressure drop in the flow channels (by optimizing channel cross section, length, and smoothness), and minimization of heat loss to the surroundings (by using an acrylic plastic to make the cell).

Three flow channels were engraved in each of two acrylic blocks that make up the feed and permeate semi-cells. Each channel is 2 mm wide, 3 mm deep, and 200 mm long; and the total active membrane area for mass transfer is 12 cm^2. The relatively small cross-sectional area of the feed and permeate channels allows operation of the system at Reynolds Numbers higher than 10,500 while maintaining low (approximately 10 kPa (0.1 atm)) pressure drop along the channels.

Feed solution was continuously pumped from a feed reservoir (Water Bath 284, Precision Scientific, Winchester, VA) through the vertically oriented membrane cell and back to

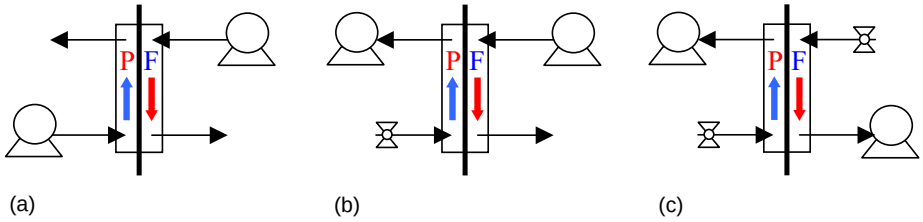

Fig. 3. DCMD configurations: (a) traditional, (b) vacuum on the permeate side, (c) vacuum on both sides.

Table 1
Membrane properties

Membrane	Material	Nominal pore size (μm)	Porosity (%)	Thickness (μm)	Active layer thickness (μm)
PS22	PP	0.22	70	150	150
TS22	PTFE	0.22	70	175	5–10
TS45	PTFE	0.45	70	175	5–10
TS1.0	PTFE	1.0	70	175	5–10

the reservoir. The water bath was constantly heated to within ±0.5 °C of the desired feed temperature. Distilled deionized water was similarly recirculated in the product loop and was cooled to within ±0.5 °C of the desired permeate temperature with a heat exchanger fed by a water chiller (ISOTEMP 1023S, Fisher Scientific, Pittsburgh, PA). The product reservoir is a 2 l filtration flask that allows overflow of excess permeating water into a collecting flask. The overflow is continuously weighed on an electronic balance (PJ360 Deltarange, Mettler Instrument Corp., Hightstown, NJ) and the permeate conductivity is continuously monitored using a conductivity meter (Model 4320, Jenway LTD., Essex, UK). Both pumps (Model 1605A, Procon Pumps, Murfreesboro, TN) are capable of delivering up to 2.7 l/min and operating at temperatures up to 70 °C. Stream temperatures are measured at the inlets and outlets of the membrane cell using two T-type dual-channel digital thermocouple thermometers (Model 600–1040, Barnant Comp., Barrington, IL). Pressures are measured at the same locations using diaphragm pressure gauges or vacuum gauges (Fisher Scientific, Pittsburgh, PA), depending on the configuration of the system. The flow rates are measured with rotometers (K71, King Instrument Comp., Huntington Beach, CA) on each side of the membrane, before or after the membrane cell, depending on the configuration of the system. The feed and permeate flow rates were kept similar at all times.

2.3. Membrane performance experiments

Membrane coupons were cut from dry flat sheets and were installed in the membrane cell. The feed solution was prepared and heated to the desired temperature and the permeate water was cooled to 20 °C. The system was then turned on and allowed to run until temperatures, pressures, and flow rates reached a steady state. When vacuum was induced, pressure and flow rate were simultaneously adjusted by two valves—a bypass valve and a front-pressure valve installed at the cell inlet. Flow rate on a membrane side that was run without vacuum was adjusted only by a bypass valve—leaving the front-pressure valve completely open. Temperatures, pressures, and flow rates were continuously monitored and controlled; cumulative overflow and permeate conductivity were recorded every 15 min up to an average period of 2 h or until the system showed stable performance. Permeate flux and salt rejection were calculated from the recorded data and the test was completed when flux was constant for at least 30 min.

2.4. Solution chemistry

Certified ACS grade NaCl (Fisher Scientific, Pittsburgh, PA) and synthetic seawater salt (Instant Ocean® Synthetic Sea Salts, Aquarium Systems, Inc., Mentor, OH) were used as the solutes in the experiments. In the DCMD experiments that did not involve investigation of feed concentration effects, the feed water was dosed with 0.6 g/l NaCl. In the DCMD experiments that tested the effect of feed concentration on the performance of the process, sodium chloride or synthetic sea salt in the range of 0.6–73 g/l was added to the feed water and the conductivity of the permeate was continuously monitored.

3. Results and discussion

3.1. Traditional DCMD

Three sets of experiments were carried out in a traditional DCMD configuration in order to acquire baseline performance data to compare with the new configurations as well as with earlier investigations of DCMD. These experiments evaluated the effects of stream velocity, temperature difference across the membrane, and system positive pressure on the flux of water vapors.

3.1.1. Effect of stream velocity on flux

Fig. 4 illustrates the performance of the four membranes investigated as a function of feed and permeate stream velocities. These experiments were performed with feed and permeate temperatures of 40 and 20 °C, respectively, and a feed salt concentration of 0.6 g/l NaCl. Salt rejection was greater than 99.9% throughout all the experiments. Results indicate that flux increases with increasing flow velocity. This was expected due to enhanced mixing in the flow channel and a decrease in the thickness of the temperature boundary layer [18,38,39]. Results also show that for the composite membranes (TS1.0, TS45, and TS22) flux increases with increasing pore size. This was also expected, simply because with increasing pore size, mass transfer in the pores is no longer controlled by mostly Knudsen diffusion but by Knudsen-viscous transition that results in increased permeability and therefore a higher flux [23,29].

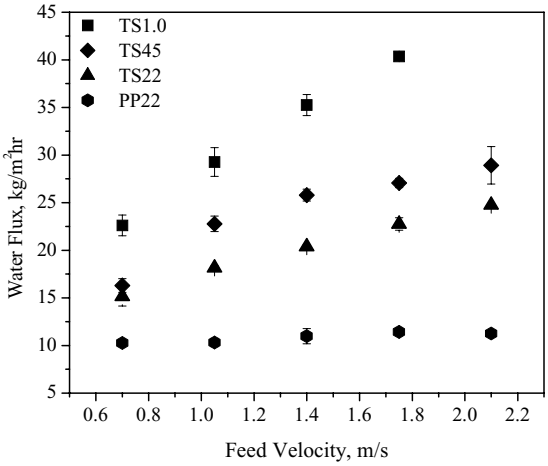

Fig. 4. Flux vs. feed velocity in traditional DCMD. Feed and permeate temperatures are 40 and 20 °C, respectively; feed salt concentration is 0.6 g/l NaCl.

The symmetric, isotropic membrane (PP22) had lower flux values than the TS22 even though both have the same pore size. This is most likely due to its thicker structure that imposes higher resistance to vapor diffusion in the pores and results in lower permeability [18,23].

Experiments with the 1.0 μm PTFE membrane were performed only in this part of the research. Despite its impressive flux at relatively low temperatures, its salt rejection deteriorated very rapidly, falling below 98.0% when stream velocity was raised above 1.75 m/s. This behavior is anticipated for membranes with larger pore size in which the LEPW is very low (below 170 kPa (10 psig)) and when a significant pressure is required to generate a high enough flow rate in the flow channel [23,40]. These two occurrences lead to flooding of the pores and passage of salt to the permeate stream.

3.1.2. Effect of feed temperature on flux

Fig. 5 illustrates the performance of the remaining three membranes at different temperature gradients across the membrane. The permeate stream temperature was maintained at 20°C and feed and permeate stream velocities were both maintained at 1.75 m/s. Salt rejection was always greater than 99.8%. The fluxes of the TS45 and TS22 exhibit an exponential dependence on temperature—as would be expected when considering the Antoine equation for vapor pressure of water:

$$p = \exp\left(23.238 - \frac{3841}{T - 45}\right) \tag{4}$$

where p is the vapor pressure of water in Pa and T is the temperature in K.

The flux through the PP22 membrane increased linearly with temperature. This behavior is most likely due to the more significant effect of the membrane thickness over the thermodynamic effects. In modeling mass transfer in MD, it is well established that the permeability coefficient is a function of the reciprocal of the membrane thickness [23]:

$$N \propto \frac{r^{a}\varepsilon}{\tau\delta} \tag{5}$$

where N is the permeability coefficient, r the membrane pore size, α a diffusion parameter, ε the membrane porosity, τ the pore tortuosity, and δ is the membrane thickness. In the current study, the PP22 membrane was substantially thicker than the TS22 membrane (symmetric versus composite membrane) and therefore the effect of the thickness at elevated temperatures overshadows the effect of the temperature on water flux. Furthermore, the PTFE membranes have rougher surfaces, especially the surface of the support layer, which might further contribute to mixing at the membrane interfaces and therefore to better performance compared to the PP membrane [41].

3.1.3. Effect of system positive pressure on flux

In the last set of traditional DCMD experiments, the effect of increased positive pressure on water flux was investigated. During early experiments, it was observed that the total pressure and pressure drop along the flow channel increased with increasing flow rates. This phenomenon is well known in channel flow [40]; however, it has not been addressed in MD studies with regard to its effect on permeate flux. Thus far, the effect of positive pressure in MD was most often discussed in the literature in the context of LEPW—concerning the risk of flooding the pores in extreme circumstances. As this study involves the inquiry of the effect of negative pressure on flux, the effect of positive pressure on flux is also important.

Fig. 6 illustrates the flux obtained with the TS45 membrane at feed and permeate temperatures of 40 and 20 °C, respectively; flow velocity of 1.05 m/s; and feed salt concentration of 0.6 g/l NaCl. The data show almost no effect of positive pressure on flux of water. These results were unexpected, especially in light of observations of later

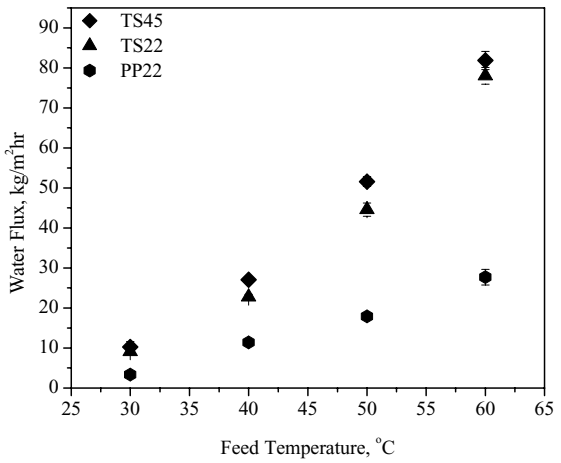

Fig. 5. Flux vs. feed temperature in traditional DCMD. Permeate temperature is 20 °C; feed and permeate velocities are 1.75 m/s; feed salt concentration is 0.6 g/l NaCl.

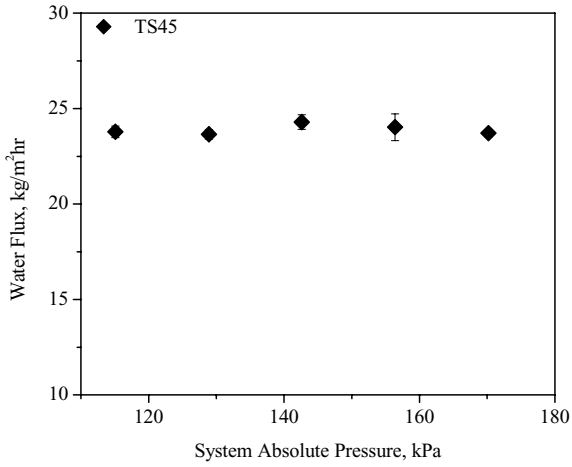

Fig. 6. Flux vs. system pressure in traditional DCMD. Feed and permeate temperatures are 40 and 20 °C, respectively; feed and permeate velocities are 1.05 m/s, and feed salt concentration is 0.6 g/l NaCl.

experiments with vacuum in the system. The results might be viewed as the sum of two competing effects—increased flux due to compaction of the membrane and decreased flux due to increased air pressure in the pores that increases the resistance to vapor transport. The significance of these results implies that operating traditional DCMD processes at pressures up to the LEPW (135–400 kPa) only minimally affects the mass transport of water vapors across the membrane.

3.1.4. Overall performance in traditional DCMD mode

Overall, results in the traditional DCMD mode were exceptionally high and exceeded results obtained in earlier studies published in the literature with similar membrane pore size and operating conditions. The independent variable chosen to compare these studies was Reynolds Number at two different feed temperatures. Reynolds Number, as an indicator of mixing intensity, is also a good representation of normalized operating conditions in MD. The hollow points in Fig. 7 represent the highest fluxes previously reported in the literature for 0.22 μm membranes (Fig. 7a) and 0.45 μm membranes (Fig. 7b). The solid points are results obtained in the current study using the 0.22 μm PTFE membrane (TS22) at 40 and 60 °C (Fig. 7a) and the 0.45 μm PTFE membrane (TS45) at 40 and 60 °C (Fig. 7b) in traditional DCMD configuration. The highest fluxes reported in previous investigations of 0.22 μm pore size membranes [2,5,6,10,11,26,42–49] at 40 and 60 °C were approximately 13.5 and 41.1 kg/(m^2 h), respectively. The highest fluxes of the 0.22 μm membrane in the current investigation (traditional DCMD configuration) were 24.7 and 81.5 kg/(m^2 h) for 40 and 60 °C, respectively. This represents flux improvement of almost 100%. Similar improvement can be seen when comparing previously reported results [14,18,26,43,50,51] with current results for the 0.45 μm pore size membrane (Fig. 7b).

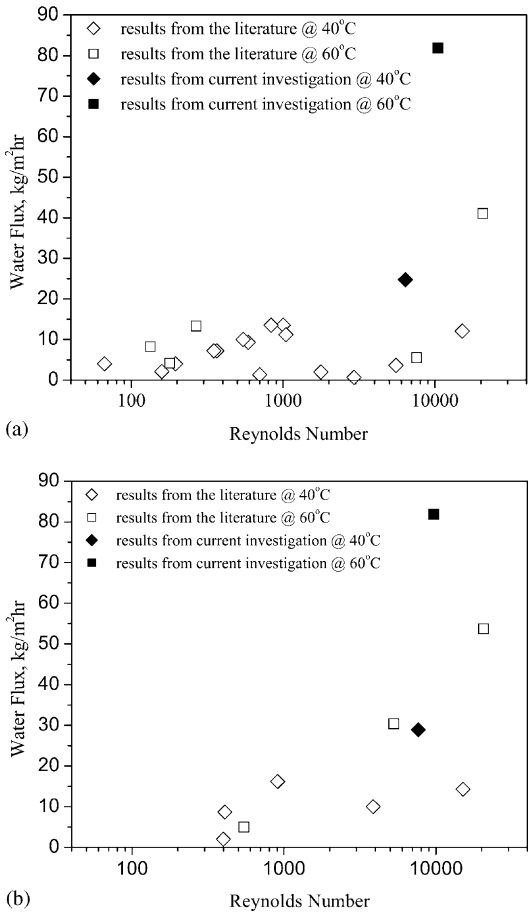

Fig. 7. Survey of previous MD studies with (a) 0.22 μm and (b) 0.45 μm hydrophobic membranes.

The improved performance can be attributed to several factors. High mixing in the thermal boundary layers of the membrane improves the convective heat transfer and thereby maintains high temperature polarization across the membrane. The use of acrylic plastic (which has a low conductive heat transfer coefficient) as the construction material of the membrane cell reduces the heat loss from the system. In addition, utilization of composite membranes with very thin active layers induces very low resistance to mass transfer of vapors through the pores. The combination of these factors resulted in fluxes that are 2–30 times higher than previous investigations.

3.2. The new DCMD/vacuum configuration

After collecting traditional DCMD baseline data, the configuration of the test unit was modified so that the permeate stream was flowing under a slight negative pressure. Fig. 8 illustrates the flux changes that occur when permeate pressure is switched from slightly positive pressure (108 kPa) in the traditional configuration to slightly negative pressure (94 kPa) in the DCMD/vacuum configuration. The flow velocity was varied from 0.7 to 2.1 m/s, and the feed and permeate temperatures were 40 and 20 °C, respectively. Experiments revealed a flux increase of up to 15% compared to results obtained using traditional DCMD at similar temperatures. Theoretically and practically this change involves no additional investment of energy in the process (when considering power consumption as the multiplication of pressure and flowrate). Thus, the modified system results in a “free” gain of up to 15% in flux.

Fig. 9 illustrates the effect of further deepening of the vacuum on the permeate side of the membrane. This was accomplished by restricting the flow on the permeate side with the front pressure valve (Fig. 3b) and adjusting the flow rate with the cell bypass valve (Fig. 1). All experiments using this configuration were performed with feed and permeate temperatures of 40 and 20 °C, respectively; feed and permeate flow velocities of 1.4 m/s; and a feed salt concentration of 0.6 g/l NaCl. Salt rejection of all three membranes was always greater than 99.8%. Deepening of the vacuum on the permeate side results in a linear increase in the flux of water for the three membranes investigated. When compared to the traditional DCMD configuration (at 108 kPa), water flux

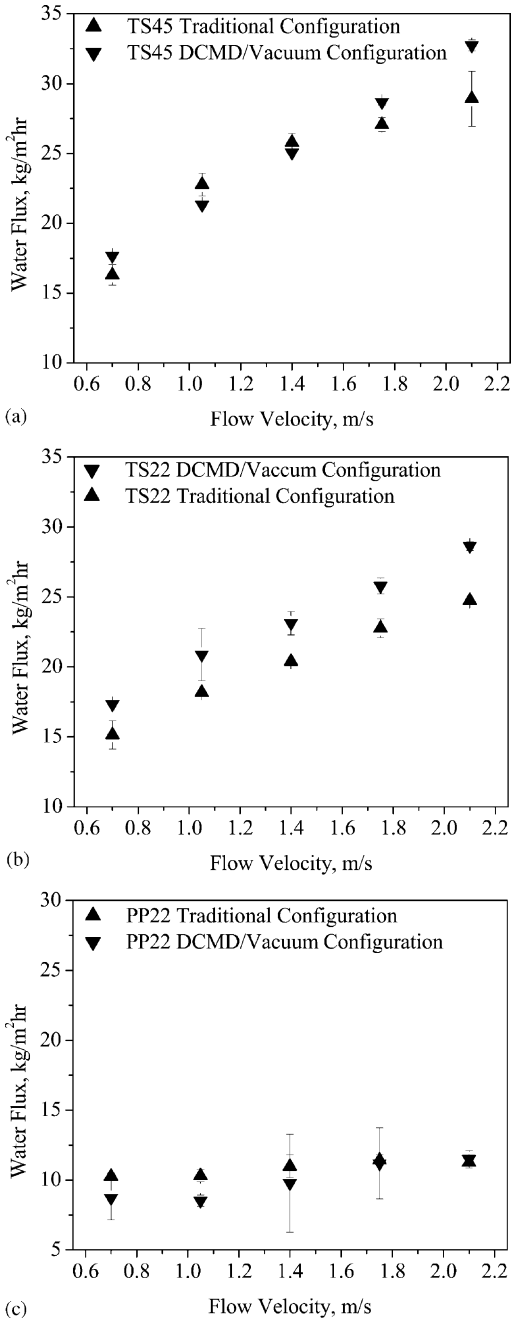

Fig. 8. Comparison of positive permeate pressure (traditional configuration) and negative permeate pressure (DCMD/vacuum configuration) on flux at various feed and permeate velocities for the (a) TS45 (b) TS22 and (c) PP22 membranes. Feed and permeate temperatures are 40 and 20 °C, respectively; absolute permeate pressures are 94 and 108 kPa; and feed salt concentration is 0.6 g/l NaCl.

for the deepest vacuum investigated (55 kPa) increased up to 84%. A similar linear trend was also observed and modeled by Schofield et al. [17,18] who systematically investigated the effect of vacuum on the performance of DCMD. However, Schofield et al. predicted much lower flux increases over a wide range of pressures and temperatures due to adverse effects of temperature polarization in the module.

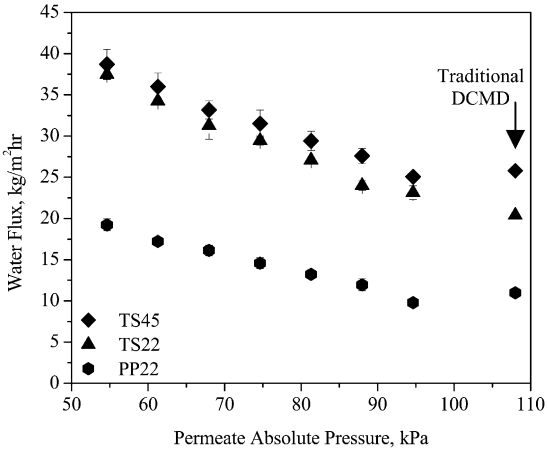

Fig. 9. Effect of permeate side vacuum on flux of water in the DCMD/vacuum configuration. Feed and permeate temperatures are 40 and 20 °C, respectively; feed and permeate velocities are 1.4 m/s; and feed salt concentration is 0.6 g/l NaCl. The reported pressure is at the inlet of the permeate side.

The enhanced fluxes shown in Figs. 8 and 9 are the result of enhanced mixing in the membrane cell channels—which mitigates temperature polarization effects across the membrane; partial elimination of stagnant air from the pores—air that poses increased resistance to the flow of vapors across the membrane; increased convective mass transport in the pores due to the increase of the total pressure gradient in the pore; and reduced conductive heat loss through the membrane cell. Based on results from the traditional DCMD configuration, the flux could have been even further increased in the DCMD/vacuum configuration by increasing the feed flow rate at the same temperature and pressure differences across the membrane.

3.3. Effect of high salt concentration on enhanced DCMD configuration

Fig. 10 illustrates the effect of increasing feed salt concentration on the performance of the DCMD/vacuum configuration. Feed NaCl (a) or sea salt (b) concentration was varied from 0.6 to 73 g/l. Feed and permeate temperatures were 40 and 20 °C, respectively; feed and permeate flow velocities were kept at 1.4 m/s; and the permeate pressure was arbitrarily chosen as 68 kPa at the inlet to the permeate side of the membrane cell. Results of experiments with NaCl show an average flux decline of 9% over the investigated range. Performance was similar with the synthetic sea salt (Fig. 10b)—an average of 9% flux decline was observed in the three membranes when sea salt concentration was increased from 0.6 to 73 g/l. In all cases, both salt and sea salt rejection was higher than 99.85%, with the majority greater than 99.9%.

Dissolved compounds reduce the vapor pressure of a solvent in aqueous solution [52]. Therefore, as the salt concentration in the feed stream of MD processes increases, the

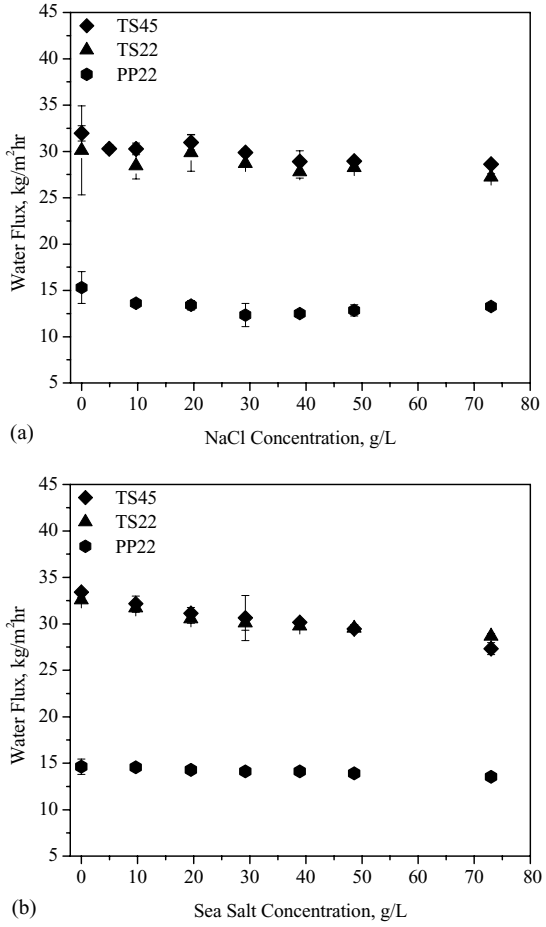

Fig. 10. Effect of (a) NaCl and (b) sea salt concentrations in the feed on flux in the DCMD/vacuum configuration. Feed and permeate temperatures are 40 and 20 °C, respectively; feed and permeate velocities are 1.4 m/s; and permeate absolute pressure is 69 kPa.

vapor pressure of the water decreases and results in a lower driving force for evaporation. Correspondingly, Wang et al. [53,54] demonstrated that if salt concentration in the permeate stream is increased, flux will be increased due to reduced vapor pressure in the permeate—a phenomenon used in the osmotic distillation process.

When salts are present in the feed solution at high concentration, an additional boundary layer develops next to the membrane interface, parallel to the temperature and velocity boundary layers. This concentration boundary layer, together with the temperature boundary layer further reduces the driving force for evaporation. Enhanced turbulence in the feed stream reduces both boundary layers and improves DCMD performance. Lawson and Lloyd [26] observed that concentration polarization had almost no effect on water flux over extended ranges of temperatures (40–80 °C) and feed concentrations (0–1.3 mol%) when strong mixing was maintained in the feed stream.

One of the most significant advantages of the DCMD process for desalination is the relatively minimal effect of feed salt concentration on the performance of the system. In reverse osmosis (RO) operations, increased feed salt concentration can substantially reduce the driving force for mass transfer across the membrane [55,56] and increase the salt passage through the membrane [57,58]. The operating conditions in RO promote concentration polarization, scaling, compaction of a cake layer, and increased osmotic pressure that leads to reduced performance. In DCMD, increased feed salt concentration only marginally decreases the vapor pressure of water. To illustrate this, assume a feed solution of 70 g/l NaCl (~7.6 wt.%) and an RO system operating at 5.6 MPa (800 psig). Neglecting concentration polarization effects, the driving force in the RO system would drop by more than 85% when the feed concentration is raised from pure water to 70 g/l NaCl. In DCMD, Raoult's Law of partial pressures predicts that the vapor pressure of the water in the solution would drop by slightly more than 2%.

Results at 73 g/l NaCl showed a flux decline of approximately 9%. The resulting 7% difference between the observed flux decline and the theoretical 2% decline in driving force is most likely due to the effects of concentration polarization at the feed–membrane interface. Results in other studies [2,7,10,18,43,59] have shown total flux declines of 13–28% for MD systems operated with feed concentrations of 30–120 g/l NaCl.

Concentration polarization effects are present in both processes and tend to lower the driving force. In RO processes, concentration polarization increases the osmotic pressure at the membrane surface, thereby decreasing the driving force for mass transport. In DCMD, concentration polarization decreases the partial vapor pressure of water at the feed–membrane interface, thereby only slightly reducing the driving force for evaporation. Furthermore, the pressure in RO may decrease flux due to compaction of the concentration boundary layer and due to slower shear flow [60]; the absence of pressure in DCMD together with high turbulence likely mitigates the effect of concentration polarization on the performance of the desalination process [23].

3.4. DCMD with vacuum on both sides of the membrane (DCMD/vacuum–vacuum)

The main objective in testing the third configuration was to separate the effect of convective mass transport due to the total pressure gradient across the membrane and the effect of reduced resistance to mass transport in the pores due to the partial elimination of the air film in the pores. Previous studies have shown that evacuation of the entire system and operation with vacuum on both sides of the membrane increases the performance of the process [11,17,18]. Therefore, it was also worthwhile to compare previously reported MD performance under similar conditions to the DCMD/vacuum–vacuum configuration. The new configuration with vacuum on both sides of the membrane was operated in co-current mode to induce similar pressures on the opposite sides of the membrane at all points. However, since co-current flow in membrane distillation is likely to

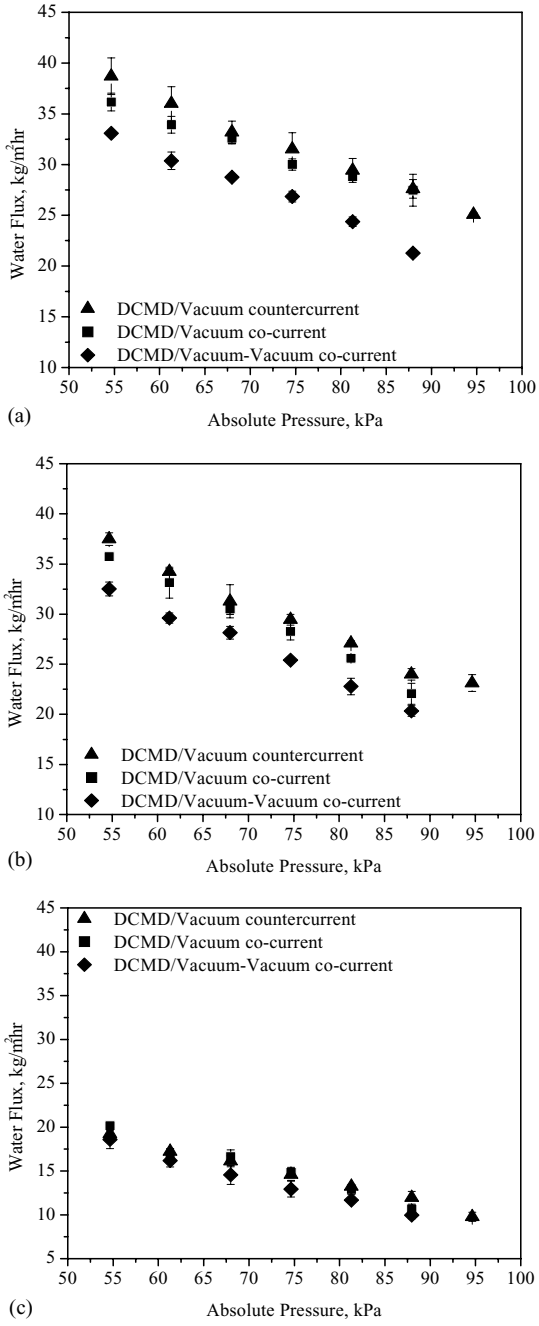

Fig. 11. Effect of flow pattern and feed-side vacuum on flux for the (a) TS45 (b) TS22 and (c) PP22 membranes. (◆) DCMD/vacuum in countercurrent mode, (■) DCMD/vacuum in co-current mode, and (▲) DCMD/vacuum–vacuum in co-current mode. Feed and permeate temperatures are 40 and 20 °C, respectively, and feed and permeate velocities are 1.4 m/s.

underperform, due to the heat exchanger behavior of the module, a set of experiments using the DCMD/vacuum configuration (without vacuum on the feed side) was conducted in co-current mode for comparison purposes. Fig. 11 shows the results of these experiments with the three membranes at feed and permeate temperatures of 40 and 20 °C, respectively, and feed and permeate velocities of 1.4 m/s. As expected, fluxes of water were slightly lower in co-current mode (■) than in countercurrent mode (▲). Moreover, operating with vacuum on both sides of the membrane (◆) led to further flux decline.

Results from experiments with the three membranes in co-current mode showed almost equal flux decline at any pressure when feed was under negative or positive pressure. Essentially, it would be expected that when the total pressure gradient increases, the secondary driving force induced by that gradient would enhance the mass transport of vapors and that the distance between the two curves (■ and ◆) would grow as the total pressure decreases. In reality, under the operating conditions investigated, this trend was not observed. Given the complexity of the different configurations and their impact on the membranes, the current behavior might be attributed to effects such as membrane compaction or swelling and their impact on membrane thickness and tortuosity, geometry of the vapor–liquid interfaces at the pore entrances, and other physical effects. Nevertheless, from the energetic standpoint, comparing the two configurations (■ and ◆) indicates that more flux can be extracted in the process with lower energy invested.

Flux of water vapors through the PP membrane is highly controlled by the thickness of the membrane. Similar to all previous results in the current study, the effects of improved operating conditions are hindered by the properties of the membrane and very little improvement in mass transport is detected (Fig. 11c).

3.5. Economic benefits

Although it is difficult to estimate full-scale performance based on bench scale results, a few points on the economics of the enhanced DCMD process compared to an RO process can be highlighted. Pilot scale tests with a large membrane module operated in enhanced DCMD mode would provide more accurate data for economic analysis.

When examining the manufacturers' performance data of commercial RO elements for seawater desalination, the reported range of flux is 18–34 l/(m^2 h) [61–63]. Considering that the flux in most RO elements is lower than the stated one due to concentration polarization effects, enhanced DCMD with more than 35 l/(m^2 h) (at 40 °C feed temperature) is a considerable advantage. Furthermore, results in the current study (Fig. 5) show that flux increases by more than 2 l/(m^2 h) for every 1 °C increase in feed temperature.

One of the most significant advantages of the DCMD process for desalination is the relatively minimal effect of feed salt concentration on the performance of the system (Fig. 10). In DCMD, increased feed salt concentration only marginally decreases the vapor pressure of water and therefore minimally decreases the driving force for mass transfer. In RO, increased feed salt concentration significantly decreases the driving force for mass transport and also increases salt passage through the membrane.

If a DCMD desalination plant is operated in conjunction with a power plant or any other source of waste heat, the cost of energy for heating the feed water is negligible and the thermally polluted water is used beneficially. Other sources of energy such as renewable solar or geothermal energy could be utilized to heat the feed water [2,5,9]. As opposed to warm condenser water, use of renewable sources would involve higher capital investment. However, this investment may eventually be paid off by lower operating costs.

Although DCMD requires two pumps for operation, one for the feed and one for the permeate, lower pressures are required compared to the high pressures required for RO operation. Low pressure pumps are less expensive in both capital and operating costs. If the enhanced DCMD configuration is employed, a vacuum permeate pump would be utilized, however, the operating costs would still be low due to the low pressure gradient on the pump.

The stated permeate recovery of a single RO element is 10–15%. The results of the current bench scale tests showed recoveries that are much lower than 1%. However, it is expected that with scaling up the enhanced DCMD module, permeate recovery will rise to a more reasonable level.

Membrane cleaning is a major consideration in operating membrane treatment processes, and making membranes more chemically resistant to cleaning agents is crucial [64]. MD membranes are made of chemically resistant polymers and can tolerate chlorine and other oxidizing agents—making them more durable and reducing membrane replacement needs.

4. Conclusions

A new approach for the design and operation of DCMD for desalination was investigated. It was demonstrated that careful design of a membrane module and configuration of the MD system could simultaneously reduce temperature polarization and permeability obstructions in the DCMD of salt solutions. Result have shown that extraordinary fluxes can be achieved and that flux can be more than doubled compared to the traditional mode of DCMD operation at relatively low temperatures. Rejection of salts is always high in MD processes and is not affected by the concentration of salt in the feed solution. Future research in nanotechnology sciences promises to generate new materials and surfaces with uniform straight pores in the nanoscale size. This would further optimize membrane permeability and further improve the MD process [35].

Acknowledgements

The authors would like to especially thank Mrs. Dita and Mr. Lucian Bronicki for their guidance and support. The authors thank Dr. Steven Kloos from Osmonics Inc. for his technical advice and for providing the membranes for this research. The authors would also like to thank Jeff Curtis, Catie Heine, Wade Cline, Walt Weaver, and Bill Cobb at the University of Nevada, Reno for their dedicated technical assistance.

References

[1] S.I. Anderson, N. Kjellander, B. Rodesjö, Design and field tests of a new membrane distillation desalination process, Desalination 56 (1985) 345.
[2] F.A. Banat, R. Jumah, M. Garaibeh, Exploitation of solar energy collected by solar stills for desalination by membrane distillation, Renewable Energy 25 (2002) 293.
[3] L. Basini, G. D'angelo, M. Gobbi, G.C. Sarti, A desalination process through sweeping gas membrane distillation, Desalination 64 (1987) 245.
[4] L. Carlsson, The new generation in sea water desalination: SU membrane distillation system, Desalination 45 (1983) 221.
[5] P.A. Hogan, Sudjito, A.G. Fane, G.L. Morrison, Desalination by solar heated membrane distillation, Desalination 81 (1991) 81.
[6] S.T. Hsu, K.T. Cheng, J.S. Chiou, Seawater desalination by direct contact membrane distillation, Desalination 143 (2002) 279.
[7] L. Martinez-Diez, F.J. Florido-Diez, Desalination of brines by membrane distillation, Desalination 137 (2001) 267.
[8] G.C. Sarti, C. Gostoli, S. Matulli, Low energy cost desalination processes using hydrophobic membranes, Desalination 56 (1985) 277.
[9] J. Walton, S. Solis, H. Lu, C. Turner, H. Hein, Membrane distillation desalination with a salinity gradient solar pond, 1999, http://rorykate.ce.utep.edu/Projects/1999MembraneTechConf/1999-17thAnnualMembrneTechConf.htm.
[10] D. Wirth, C. Cabassud, Water desalination using membrane distillation: comparison between inside/out and outside/in permeation, Desalination 147 (2002) 139.
[11] A.G. Fane, R.W. Schofield, C.J.D. Fell, The efficient use of energy in membrane distillation, Desalination 64 (1987) 231.
[12] J.M.O.D. Zarate, A. Velazquez, L. Pena, J.I. Mengual, Influence of temperature polarization on separation by membrane distillation, Sep. Sci. Technol. 28 (1993) 1421.
[13] M. Sudoh, K. Takuwa, H. Iizuka, K. Nagamatsuya, Effects of thermal and concentration boundary layers on vapor permeation in membrane distillation of aqueous lithium bromide solution, J. Membr. Sci. 131 (1997) 1.
[14] L. Martinez-Diez, F.J. Florido-Diez, M.I. Vazquez-Gonzalez, Study of polarization phenomena in membrane distillation of Aqueous salt solutions, Sep. Sci. Technol. 35 (2000) 1485.
[15] S.P. Agashichev, A.V. Sivakov, Modeling and calculation of temperature-concentration polarization in the membrane distillation process, Desalination 93 (1993) 245.
[16] R.W. Schofield, A.G. Fane, C.D.J. Fell, Gas and vapor transport through microporous membrane. I. Knudsen-Poiseulle transition, J. Membr. Sci. 53 (1990) 159.
[17] R.W. Schofield, A.G. Fane, C.D.J. Fell, Gas and vapor transport through microporous membrane. II. Membrane distillation, J. Membr. Sci. 53 (1990) 173.
[18] R.W. Schofield, A.G. Fane, C.D.J. Fell, Factors affecting flux in membrane distillation, Desalination 77 (1990) 279.
[19] R.W. Schofield, A.G. Fane, C.D.J. Fell, Heat and mass transfer in membrane distillation, J. Membr. Sci. 33 (1987) 299.
[20] M. Gryta, M. Tomaszwska, Heat transport in the membrane distillation process, J. Membr. Sci. 144 (1998) 211.
[21] B. Gebhart, Heat Conduction and Mass Diffusion, McGraw-Hill, New York, NY, 1993.

[22] S. Bandini, C. Gostoli, G.C. Sarti, Role of heat and mass transfer in membrane distillation process, Desalination 81 (1991) 91.
[23] K.W. Lawson, D.R. Lloyd, Review: membrane distillation, J. Membr. Sci. 124 (1997) 1.
[24] A. Burgoyne, M.M. Vahdati, Direct contact membrane distillation—review, Sep. Sci. Technol. 35 (2000) 1257.
[25] K.W. Lawson, D.R. Lloyd, Membrane distillation. I. Module design and performance evaluation using vacuum membrane distillation, J. Membr. Sci. 120 (1996) 111.
[26] K.W. Lawson, D.R. Lloyd, Membrane distillation. II. Direct contact membrane distillation, J. Membr. Sci. 120 (1996) 123.
[27] L. Martinez-Diez, M.I. Vazquez-Gonzalez, Study of membrane distillation using channel spacers, J. Membr. Sci. 144 (1998) 45.
[28] K. Schneider, T.J. van Gassel, Membrane distillation, Chem. Eng. Technol. 56 (1984) 514.
[29] C.M. Guijt, I.G. Rácz, J.W.T. Reith, A.B. de Haan, Determination of membrane properties for use in the modelling of a membrane distillation module, Desalination 132 (2000) 255.
[30] K.S. McGuire, K.W. Lawson, D.R. Lloyd, Pore size distribution determination from liquid permeation through microporous membrane, J. Membr. Sci. 99 (1995) 127.
[31] K.W. Lawson, M.S. Hall, D.R. Lloyd, Compaction of microporous membrane used in membrane distillation. I. Effect on gas permeability, J. Membr. Sci. 101 (1995) 99.
[32] H. Reulen, C.A. Smolders, G.F. Versteeg, Determination of mass transfer rates in wetted and non wetted microporous membranes, Chem. Eng. Sci. 48 (1993) 2093.
[33] A.C.M. Franken, J.A.M. Nolten, M.H.V. Mulder, Wetting criteria for the applicability of membrane distillation, J. Membr. Sci. 33 (1987) 315.
[34] M.C. García-Payo, M.A. Izquierdo-Gil, C. Fernández-Pineda, Wetting study of hydrophobic membranes via Liquid entry pressure measurements with aqueous alcohol solutions, J. Colloid Interface Sci. 230 (2000) 420.
[35] S.B. Sinnott, Computational Studies of Carbon Nanotube-Based Membranes and New Materials, Eighth Foresight Conference on Molecular Nanotechnology, Bethesda, Maryland, 3–5 November 2000.
[36] Material Information: Polypropylene, 2002, http://www.goodfellow.com/static/E/PP30.HTML.
[37] Thermal properties: PVDF, 2002, http://www.ausimont.com/docs/hylar_therm.html.
[38] J.P. Holman, Heat Transfer, sixth ed., McGraw-Hill, New York, NY, 1986.
[39] W.M. Kays, M.E. Crawford, Convective Heat and Mass Transfer, third ed., McGraw-Hill, New York, NY, 1993.
[40] J.G. Knudsen, D.L. Katz, Fluid Dynamics and Heat Transfer, McGraw-Hill, New York, NY, 1980.
[41] W.M. Rohsenow, J.P. Hartnett, Y.I. Cho, Handbook of Heat Transfer, third ed., McGraw-Hill, New York, NY, 1998.
[42] M. Gryta, M. Tomaszwska, J. Grzechulska, A.W. Morawski, Membrane distillation of NaCl solution containing organic matter, J. Membr. Sci. 181 (2001) 279.
[43] L. Martínez-Díez, F.J. Florido-Díaz, M.I. Vázquez-González, Study of evaporation efficiency in membrane distillation, Desalination 126 (1999) 193–198.
[44] P.P. Zolotarev, V.V. Ugrozov, I.B. Volkina, V.N. Nikulin, Treatment of wastewater for removing heavy metals by membrane distillation, J. Hazard. Mater. 37 (1994) 77.
[45] A. Burgoyne, M.M. Vahdati, G.H. Priestman, Investigation of flux in flat-plate modules for membrane distillation, Dev. Chem. Eng. Miner. Process. 3 (1995) 161.
[46] P. Godino, L. Pena, J.I. Mengual, Membrane distillation: theory and experiments, J. Membr. Sci. 121 (1996) 83.
[47] S.P. Rudobashta, I.B. Elkina, Diffusive permeation of vapor in membrane distillation, Theor. Found. Chem. Eng. 33 (1999) 363.
[48] M. Gryta, Direct contact membrane distillation with crystalization applied to NaCl solution, Chem. Pap. 56 (2002) 14.
[49] F.A. Banat, F.A.A. Al-Rub, R. Jumah, M. Al-Shannag, Modeling of desalination using tubular direct contact membrane distillation modules, Sep. Sci. Technol. 34 (1999) 2191.
[50] L. Martinez, F.J. Florido-Diaz, Theoretical and experimental studies on desalination using membrane distillation, Desalination 139 (2001) 373.
[51] M. Gryta, M. Tomaszwska, A.W. Morawski, Membrane distillation with laminar flow, Sep. Purif. Technol. 11 (1997) 93.
[52] T.L. Brown, J.H.E. LeMay, B.E. Bursten, Chemistry: the Central Science, seventh ed., Prentice-Hall, Upper Saddle River, NJ, 1997.
[53] Z. Wang, F. Zheng, S. Wang, Empirical study of membrane distillation with brine circulated in the cold side, J. Membr. Sci. 183 (2001) 171.
[54] Z. Wang, F. Zheng, Y. Wu, S. Wang, Membrane osmotic distillation and its mathematical simulation, Desalination 139 (2001) 423.
[55] S. Bhattacharya, S.T. Hwang, Concentration polarization, J. Membr. Sci. 132 (1997) 73.
[56] E.M. Vrijenhoek, S. Hong, M. Elimelech, Influence of membrane surface properties on initial rate of colloidal fouling of reverse osmosis and nanofiltration membranes, J. Membr. Sci. 188 (2001) 115.
[57] G. Jonsson, Overview of theories for water and solute transport in UF/RO membranes, Desalination 35 (1980) 21.
[58] S.M.S. Ghiu, R.P. Camahan, M. Barger, Permeability of electrolytes through a flat RO membrane in a direct osmosis study, Desalination 144 (2002) 387.
[59] L. Martinez-Diez, M.I. Vazquez-Gonzalez, A method to evaluate coefficients affecting flux in membrane distillation, J. Membr. Sci. 173 (2000) 225.
[60] J. Mallevialle, P.E. Odendaal, M.R. Wiesner, Water Treatment Membrane Processes, McGraw-Hill, New York, NY, 1996.
[61] FILMTEC^{TM} Membrane Elements PDQ Table, 2003, http://www.dow.com/liquidseps/pc/prd_film.htm.
[62] Osmonics Reverse Osmosis Membrane Elements- DS-3, High Pressure, 2003, http://www.osmonics.com/products/Page288.htm.
[63] Hydranautics' SWC Membranes—Technical Info, 2003, http://www.membranes.com/index_net.htm.
[64] J. Glater, S.K. Hong, M. Elimelech, The search for a chlorine-resistant reverse osmosis membrane, Desalination 95 (1994) 325.